Spectroscopic Characterization of the Chemical Changes Occurring in Soy Wood Composite Adhesives When Exposed to Moisture

Joseph J. Marcinko
Anthony A. Parker

Abstract

Solid-state surface attenuated total reflectance Fourier transform infrared spectroscopy (SATR-FTIR) and solid-state nuclear magnetic resonance spectroscopy (SSNMR) were used to characterize the physiochemical changes in solid soy-flour adhesives upon exposure to water. Comparisons were made between adhesives that were prepared with and without the crosslinking chemical polyamideamine-epichlorohydrin (PAE). Comparisons were also made between neat monolithic adhesive films, and adhesives that were laminated to yellow poplar (*Liriodendron tulipifera*). FTIR data revealed that the relative surface concentration of water-soluble components on neat monolithic adhesives was higher prior to water-exposure as compared with the adhesive laminated to wood. Moreover, the chemical composition of the water-soluble extract was affected by PAE. After soaking in water, the water-soluble components were observed to dissolve and disappear from the surfaces of the adhesives, as well as from the surfaces of water-soaked wood-laminate specimens. Similarly, SSNMR results corroborated with the dissolution and disappearance of the water-soluble components from the neat monolithic adhesives after water soaking. Moreover, it was discovered that the water-soluble components have a plasticization effect when PAE is used as a crosslinker. The implications of these findings as they pertain to the mechanism of adhesion will be discussed.

For economic and environmental reasons, soy-based adhesives have continued to be of interest to wood composite manufacturers. However, since the patenting of these adhesives for use in wood composites in 2007, the technology has changed very little, and market growth has been minimal owing to poor moisture resistance.

To overcome the moisture-resistance problem, it would be helpful to understand more about the mechanism of how water affects the compositional chemistry of soy adhesives and how this chemistry in turn influences the adhesion mechanism. With a better understanding of the reasons for moisture-induced adhesive failures, it should become possible to test and develop chemistry-specific solutions to overcome the moisture resistance problem.

Very little spectroscopic data has been reported related to the adhesion mechanism occurring between soy adhesives and wood. In prior accounts, adhesion mechanisms have been proposed by Chaichang Li and others, but no validating spectroscopic data have been presented to test the mechanistic hypotheses (Li et al. 2004, Li and Yuan 2006, Li 2007, Watt 2008).

In other accounts, efforts were focused on studying the effects of processing and compositional-related factors on adhesive performance and moisture resistance (Frihart and Birkeland 2016, Hunt et al. 2023) These studies provide valuable insight regarding the importance of soy protein structure and its effect on adhesive performance. Our approach is to utilize these findings and to incorporate them into our studies of how water affects the compositional chemistry of soy adhesives. The objectives are to characterize the changes occurring in these soy adhesives when exposed to moisture; to better define the mechanism of

The authors are, respectively, PhD, Principal Scientist & President, Polymer Synergies, LLC, Bradenton, Florida (drjoe@polymersynergies.com [corresponding author]), and PhD, Principal Scientist & President, A.A. Parker Consulting, LLC, Bradenton, Florida (aaparkerconsulting@gmail.com). This paper was received for publication in December 2023. Article no. FPJ-D-23-00063R1.

Forest Prod. J. 74(2):143–150.
doi:10.13073/FPJ-D-23-00063

adhesion between these types of soy adhesives and wood substrates; and, with a better understanding of the chemical changes occurring, to develop technical solutions to solve the moisture resistance problem.

It is well known that the mechanism of adhesion between component members in composite structures is influenced by interfacial contributions (e.g., surface wetting and interpenetration between the components), and by bulk property contributions (e.g., viscoelastic and energy absorbing characteristics of the individual component members; Theocaris 1987, Guillemenet et al. 2002). Moreover, the achievement of good interfacial penetration between members can lead to phase mixing at the boundary and to the development of a mixed interphase with its own unique set of mechanical properties (Koenig 1999).

Solid-state surface FTIR techniques such as surface attenuated total reflectance spectroscopy (SATR) and reflection-absorption infrared spectroscopy (RAIRS) are well-established techniques for studying the compositions of solid surfaces (Parker 2002). As such, these techniques have also been useful for studying relationships between surface composition and adhesion in a variety of composite systems (Parker et al. 1992, Parker and MacLachlan 2000, Parker 2004, Bello, D. 2006). In each of these accounts, surface compositional information provided mechanistic insight pertaining to the interfacial component of the overall adhesion mechanism.

Similarly, solid-state nuclear magnetic resonance (SSNMR) techniques have also been employed in studies of composites and adhesion (Parker et al. 1993, Allen et al. 2010, Marcinko, J. et al. 2003. Thus, like FTIR, SSNMR can also be used to study the interfacial aspects of adhesion. However, because SSNMR also facilitates the study of molecular structure and molecular dynamics, it offers the opportunity to study contributions from individual components within a fully adhered composite system, thereby facilitating the study of the unique property contributions from each individual member, as well as interactions between members.

In the present study, solid state FTIR techniques were used to study the effects of moisture on the surface composition of soy-based adhesives, while SSNMR techniques were employed to study the effects of moisture on the structure and dynamics of the soy-based adhesives. The complimentary analytical strengths of each technique were combined to uncover heretofore unexplored chemistry relating to the moisture resistance of soy adhesives, and to their underlying mechanism of adhesion with wood adherends.

Experimental Methods and Materials

Monolithic soy adhesive films were prepared from a dispersion of 200/70 (mesh/PDI) soy flour in water at a 38 percent soy solids concentration (200 mesh is the particle size of the soy particles, which equates to an average particle size of 74 microns; and PDI is the Protein Dispersity Index for the soy flour, which relates to how well the soy flour disperses in water). One of the adhesive samples was prepared using a 30 percent solids polyamideamine-epichlorohydrin (PAE) resin as a crosslinker for the adhesive. The concentration of the PAE solids in the adhesive was 4 percent; thus, the final solid film consisted of 96/4 w/w soy-flour components and PAE components. This sample was labeled 67-3. A second adhesive was prepared having a 38 percent soy solids composition without PAE; thus, the final solid film consisted of 100 percent soy flour solids and was labeled 67-4.

Monolithic films of these two formula types were prepared by smearing the adhesives between two layers of nonporous aluminum foil, and then pressing the samples in a hot press at a temperature of 130°C and at a pressure of 153 pounds per square inch (PSI) for a 4-minute dwell time. After pressing, the upper foil layer was peeled away, and the adhesive films were placed in a 130°C gravity oven for an additional 10 minutes to assist in the removal of residual moisture.

In separate preparations, bilayers structures were prepared, comprising an adhesive that was laminated to a single adherend member of 0.125-inch-thick yellow poplar (*Liriodendron tulipifera*). This was done for the purpose of testing the effects of a porous wood substrate on the surface composition of the soy adhesive. The wood-laminated specimens were prepared using the same 67-3 and 67-4 adhesives that were used to prepare monolithic films.

In order to prepare the adhesive–wood bilayers, 50 grams of the wet soy-based dispersions were initially applied to a single 12- by 12-inch layer of poplar. Next, a perforated polytetrafluoroethylene (PTFE) mesh, having openings of 0.025 inches by 0.05 inch (McMaster Carr), was placed on top of the adhesive layer. A second 12- by 12-inch layer of poplar veneer was then placed on top of the PTFE mesh with the grain direction perpendicular to the bottom veneer layer. The multilayered assemblies (i.e., bottom-veneer–wet-adhesive–PTFE–top-veneer) were then pressed at 130°C for 4 minutes while under a pressure of 153 PSI.

Importantly, the porosity of the PTFE mesh facilitated the flow-through of the wet adhesive from the bottom veneer to the top veneer, thereby enabling the adhesive to penetrate the PTFE during lamination, and to make intimate contact with the upper wood veneer member. Upon completion of cure, the presence of the PTFE layer enabled facile physical separation of the laminated assembly to yield two bilayers comprising a single veneer layer laminated to an open-faced aliquot of cured adhesive. The open-faced adhesive was then used to perform surface spectroscopic studies for comparison with analogous open-faced adhesives that had been laminated to nonporous aluminum foil substrates.

The monolithic adhesive films and bilayer specimens were cut into 1-inch (2.54-cm) squares for subsequent analyses via SATR-FTIR and SSNMR. In separate experiments, specimens were subjected to an extraction–washing–drying protocol. For bilayer specimens, the top and bottom portions were placed together into single jars. For monolithic films, the samples were broken into small pieces and were placed into individual jars. Each sample was individually soaked for 3 days under ambient conditions in approximately 30 grams distilled water.

After the soak period, aliquots of the supernatants were collected with plastic pipettes and were placed into individual beakers for subsequent drying at 45 to 50°C for 24 hours. The remaining supernatants were carefully decanted from each jar, and fresh distilled water was added. After the addition of fresh water, the samples were lightly agitated, and were allowed to set for approximately 15 minutes to enable insoluble sediments to settle whenever applicable. Next, the cycle of decanting, followed by addition of fresh water, was repeated 14 additional times, for a total of 15 wash cycles. In

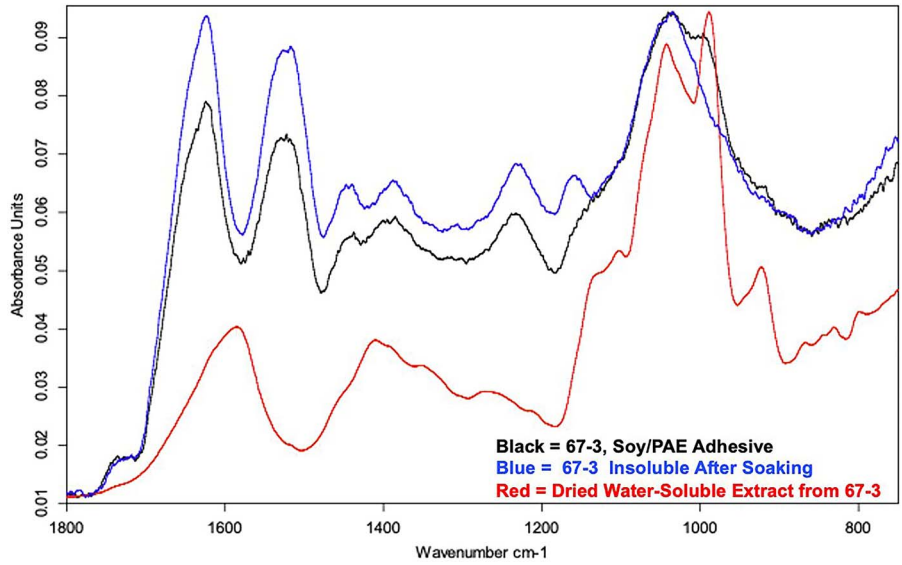

Figure 1.—Solid-state SATR spectra of the as-made soy-flour–polyamideamine-epichlorohydrin (PAE) adhesive film in black (67-3), the 67-3 insoluble residue after soaking–washing and drying in blue, and the dried water-soluble extract from the soaked 67-3 sample in red.

the final step, the bilayers and the residual insoluble fractions from the monolithic films were dried at 45 to 50°C for 24 hours. The residual insoluble components from the extracted specimens and the dried water-soluble extracts were analyzed via SATR-FTIR and SSNMR for comparison with the as-made samples prior to soaking–washing.

Solid-state SATR-FTIR studies were performed using a Bruker Alpha-P spectrometer equipped with a diamond-cell ATR accessory. Anvil pressure was applied to ensure intimate contact between the samples and the diamond crystal. Single-bounce spectra, referenced against atmospheric background spectra, were obtained under ambient conditions using signal-averaging of 36 scans at 2 cm^{-1} resolution over the spectral range 4,000 to 650 cm^{-1}. Separate spectral analyses were performed between the ranges of 1,800 to 750 cm^{-1}, 3,800 to 850 cm^{-1}, 1,200 to 850 cm^{-1}, and 1,800 to 850 cm^{-1}. The absorbance spectra were vertically maximized over the chosen spectral ranges for the purpose of enabling relative absorbance intensity comparisons among the samples.

Solid-state NMR studies were conducted at the University of Florida's National Magnet Laboratory in Gainesville, Florida, using a Bruker Avance NEO 600 spectrometer (600.76 MHz proton, 151.08 MHz carbon) with a Bruker HCN biosolids magic-angle-spinning probe. Each sample (~100 mg) was packed into a Bruker 4-mm solid-state ceramic NMR rotor with Kel-F caps. All spectra were collected with magic-angle spinning rates of 10 kHz using dry air bearing pressure, with a broadband ^{1}H decoupling field of 125 kHz during acquisition, and with ^{1}H–^{13}C cross-polarization (CP) using spin-temperature alternation of the initial ^{1}H magnetization with a 2.0 μs π/2 pulse. For CP spectra, 2,048 scans were signal-averaged under ambient conditions, and ^{1}H cross-polarization RF fields were ramped from 50 to 75 kHz while the ^{13}C cross-polarization RF field was kept constant at 62.5 kHz. In separate experiments, ^{1}H $T_{1\rho}$ relaxation rates were measured through carbon-13 using a ^{1}H spinlock RF field of 35 kHz. Twenty-one delay times were arrayed varying in time between 0 and 50 milliseconds and 1,728 scans were signal-averaged under ambient conditions, and ^{1}H $T_{1\rho}$ values were determined from single-exponential fits of carbon-13 intensity versus delay time data for each individual carbon.

Results and Discussion

Solid-state SATR-FTIR

Figure 1 shows overlayed solid-state SATR-FTIR spectra of the as-made Soy–PAE adhesive film (67-3, black trace), the 67-3 insoluble residue after soaking–washing and drying (blue trace), and the dried water-soluble extract from the soaked 67-3 sample (red trace). Note that the spectral range between 1,800 and 750 cm^{-1} was vertically maximized to a common scale using the common band at ~1,040 cm^{-1}. This facilitated comparisons of relative absorbance intensities among the co-plotted sample spectra.

The wavenumber positions of the amide-carbonyl stretching bands spanning between ~1,500 cm^{-1} to 1,650 cm^{-1} were similar both before and after soaking–washing. However, the relative intensities of the amide carbonyl bands with respect to the common band at ~1,040 cm^{-1} were observed to increase after soaking–washing. This reflects the removal of water-soluble components from the starting adhesive (i.e., the components centered at ~1,040 and ~990 cm^{-1}), which leaves an insoluble residue consisting of a higher relative concentration of protein amide-carbonyl structures.

In addition to the changes in the relative amide-carbonyl content, a water-soluble component associated with an absorption band at approximately 990 cm^{-1} was also reproducibly observed to appear on the surface of the film prior to soaking, and within the dried extract after soaking. The same band was observed to disappear from the as-made sample after soaking–washing. This band falls within the C-O stretching region of the spectrum and is likely associated with water-soluble carbohydrates that are known constituents of soy-flour (Erickson 1995).

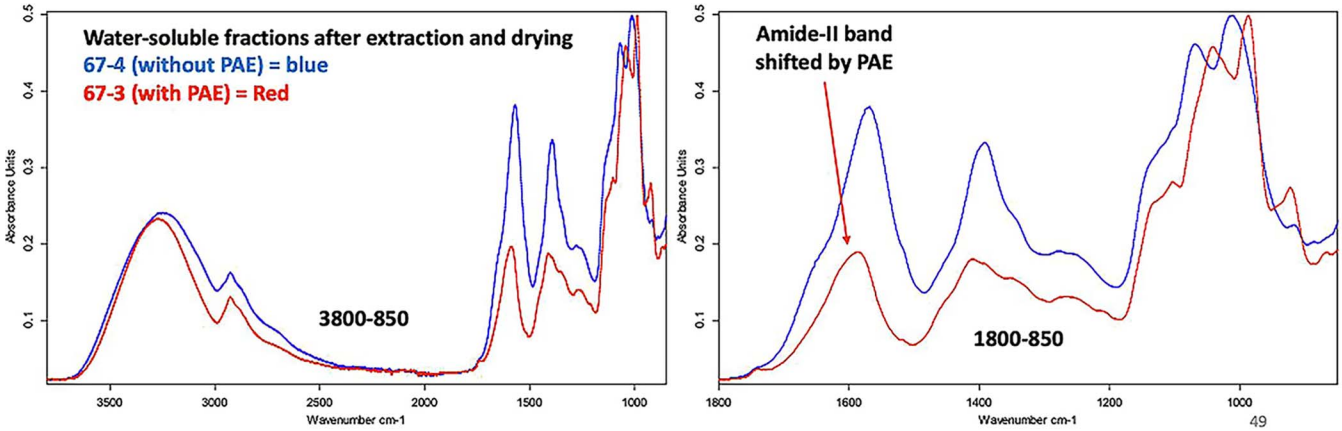

Figure 2.—Solid-state SATR-FTIR (Fourier transform infrared) spectra of dried water-soluble extracts from adhesive films 67-3 (Soy–PAE adhesive) and 67-4 (Soy adhesive without PAE) presented over the spectral range 3,800-850 cm^{-1} (left) and 1,800-850 cm^{-1} (right). The spectra were maximized to a common vertical scale using the common bands centered between ~990 and 1,040 cm^{-1}.

Importantly, although the 990 cm^{-1} band was observed to be present on the surface of the neat adhesive film as well as within the dried water-soluble extract, it was noticeably absent from the surface of the water-insoluble residue after soaking–washing and drying. Given that this band was distinctly absent from the extracted and washed solid, it follows that the portion of the adhesive associated with the 990 cm^{-1} band is water-soluble, whereas the portion of the adhesive without this band is water-resistant.

In addition, a well-defined band centered at ~1,162 cm^{-1} was also observed on the surface of the water-insoluble fraction. Like the band at 990 cm^{-1}, this band also falls within the C-O stretching region. However, in contrast to the water-soluble components associated with the 990 cm^{-1} band, the 1,162 cm^{-1} band is associated with moisture-resistant residues.

It is important to recognize that the moisture-sensitive residues were discovered to exist on the surfaces of the adhesives, where their presence might be expected to have an impact on the interfacial wetting of wood adherends as well as on the moisture resistance of the resulting interfacial bond.

Figure 2 shows the comparison of the dried water-soluble fractions extracted from monolithic films 67-3 (Soy–PAE Adhesive) and 67-4 (Soy Adhesive without PAE). Three types of distinct differences were observed. First, the relative intensities of the soluble amide moieties with respect to C-O stretching and O-H stretching moieties (~3,200 to 3,400 cm^{-1}) moieties were lower in the extract from the adhesive that was cured with PAE. This finding is also consistent with the higher relative intensities of amide-carbonyl moieties that were observed in the water-insoluble fractions of the films that were cured with PAE (Fig. 1), implying that PAE plays a role in inhibiting protein solubility.

Secondly, there was a wavenumber shift in the amide-II stretching band when PAE was used as a curing agent. In the absence of PAE, the primary amide-II maximum was observed to occur at ~1,572 cm^{-1}, whereas in the presence of PAE, the band was shifted to approximately 1,586 cm^{-1}.

Finally, the primary bands for water-soluble moieties appeared at ~1,012 cm^{-1} in the absence of PAE, and at ~990 cm^{-1} in the PAE-cured sample. A similar shift was observed for another band, which appeared at ~1,070 cm^{-1} in the absence of PAE and at about ~1,042 cm^{-1} in the presence of PAE. Collectively, these types of wavenumber shifts suggest that PAE influences the chemical composition of the water-soluble components.

When we compare the surface spectra of the 67-3 adhesive films with those from the adhesives that were laminated to wood (i.e., the surface spectra of adhesive residue on the bilayer specimens), an important similarity becomes apparent (Fig. 3). Specifically, the adhesive surfaces on the bilayer specimens were observed to contain higher relative surface concentrations of the moieties associated with the 990 cm^{-1} band prior to soaking–washing, mirroring the trend that was observed for the monolithic films. Moreover, the 990 cm^{-1} band was also observed to disappear from the surfaces after soaking–washing in water, again mirroring the behavior of the monolithic film samples.

Given that aluminum foil is nonporous, it was initially hypothesized that the water-soluble components might become physically confined by the foil during the pressing process, thereby leading to a surface with an artificially high concentration of water-soluble components. To test for this possibility, the same adhesives were purposely laminated to the porous wood veneer substrates to determine whether the water-soluble components associated with the 990 cm^{-1} band might disappear from the surfaces of the bulk adhesive via diffusion into the porous wood member during the lamination process.

However, as these results demonstrate, at least a portion of the water-soluble components at 990 cm^{-1} was observed to remain on the surfaces of the adhesives, regardless of whether they were laminated to wood or foil. Thus, we can conclusively say that the presence of water-soluble components on the surfaces of monolithic films was not entirely an artifact of the use of a nonporous foil release layer. Instead, even in the presence of a porous wood substrate, a portion of the water-soluble species remained near the surfaces of the adhesives after lamination. Given that these components of the adhesive are water-soluble as evidenced by their disappearance after soaking–washing, it follows that the moisture resistance of the bulk adhesive will likely be affected by their presence. Corroboration of these results with NMR data will be discussed below.

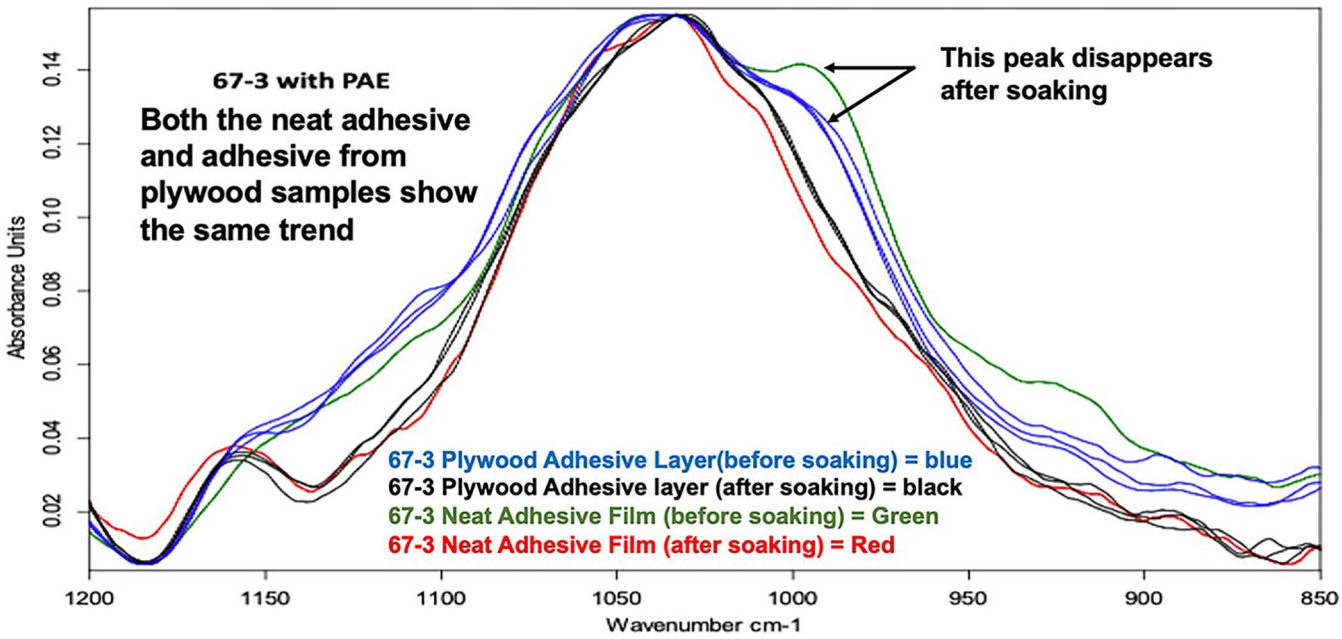

Figure 3.—Solid state SATR-FTIR spectral overlay of the C-O stretching region for 67-3 adhesive films (separated with nonporous Al-foil release layers) together with the same adhesives that were bonded to wood veneer.

Solid-state NMR

In addition to solid-state SATR-FTIR, solid-state nuclear magnetic resonance spectroscopy (SSNMR) experiments were also performed on the same solid soy adhesives samples. SSNMR techniques can facilitate the study of unique structural attributes of adhesive components, regardless of their solubility or insolubility in water. In these analyses, solid-state cross-polarized (CP) spectra of solid soy protein adhesives were acquired both before and after water-soaking–washing to probe for ^{13}C chemical shift differences that might also be associated with the types of wavenumber changes that were observed via SATR-FTIR. In addition, because NMR techniques can also be used to study molecular dynamics, proton spin lattice relaxation rates ($^{1}HT_{1\rho}$) were also measured for individual carbon atoms, for the purpose of determining whether structural changes might also be accompanied by changes in molecular, motional dynamics.

Inspection of Figure 4 reveals subtle changes that were observed in the intensities of certain peaks as well as subtle differences in the chemical shifts as a function of washing, and as a function of the presence of PAE. Specifically, independent of the presence or absence of PAE, a well-resolved resonance at ~93 parts per million (ppm) was observed to disappear from the as-made adhesive after soaking–washing and drying. Further research is underway for the purpose of identifying this component, but its chemical shift is consistent with an anomeric carbon bonded to two oxygen atoms (McBrierty and Douglass 1981). Thus, finding is consistent with the analogous disappearance of the ~990 cm^{-1} C-O stretching band that was observed via FTIR, suggesting that the water-soluble components likely comprise carbohydrates.

Another qualitative difference in the carbon-13 spectra pertains to changes in the relative intensities and resolution of resonances centered near ~72 ppm after soaking–washing. These changes were noticeably affected by the presence or absence of PAE.

In addition to the qualitative spectral differences, significant differences were also observed in molecular dynamics as measured from $^{1}HT_{1\rho}$ molecular relaxation experiments. It has been established that $^{1}HT_{1\rho}$ relaxation times are influenced by spin-diffusion and molecular motional processes (Schaefer et al. 1987, Korb and Bryant 2004). Generally, as molecular motion increases, the proton spin-diffusion process becomes less efficient, and $^{1}HT_{1\rho}$ relaxation rates increase.

Table 1 shows the $^{1}HT_{1\rho}$ relaxation data collected for the samples. When comparing the samples 67-3 and 67-4 before soaking–washing, the relaxation rates were observed to be slightly lower for 67-3 (i.e., the sample with PAE crosslinker). The differences in $^{1}HT_{1\rho}$ relaxation rates were not large, but they were outside of the window of the experimental error associated with the measurement technique. When $^{1}HT_{1\rho}$ relaxation rates decrease, this equates to an inhibition in molecular motion. Thus, from these data, we can say that PAE inhibits the molecular mobility of the adhesive molecules, as might be expected to occur from possible crosslinking reactions and network formation.

Comparison of 67-3 and 67-4 to one another after washing reveals even greater differences. Just like before washing, the sample with PAE (67-3) was less mobile than the sample without PAE (67-4), but the magnitude of the difference was even greater after soaking–washing.

In another observation, the $^{1}HT_{1\rho}$ values were observed to decrease after soaking–washing for the sample that was crosslinked with PAE (67-3). This indicates that the molecular motion of the molecules within the PAE-crosslinked lattice were attenuated upon removal of the water-soluble fraction. Said another way, when PAE is used as a crosslinking additive, the water-soluble components appear to have a plasticization effect over the adhesive matrix. Solution NMR experiments are underway to help define the chemistry responsible for this interesting observations. We speculate that the chemistry is a reaction product or degradation product between PAE and the

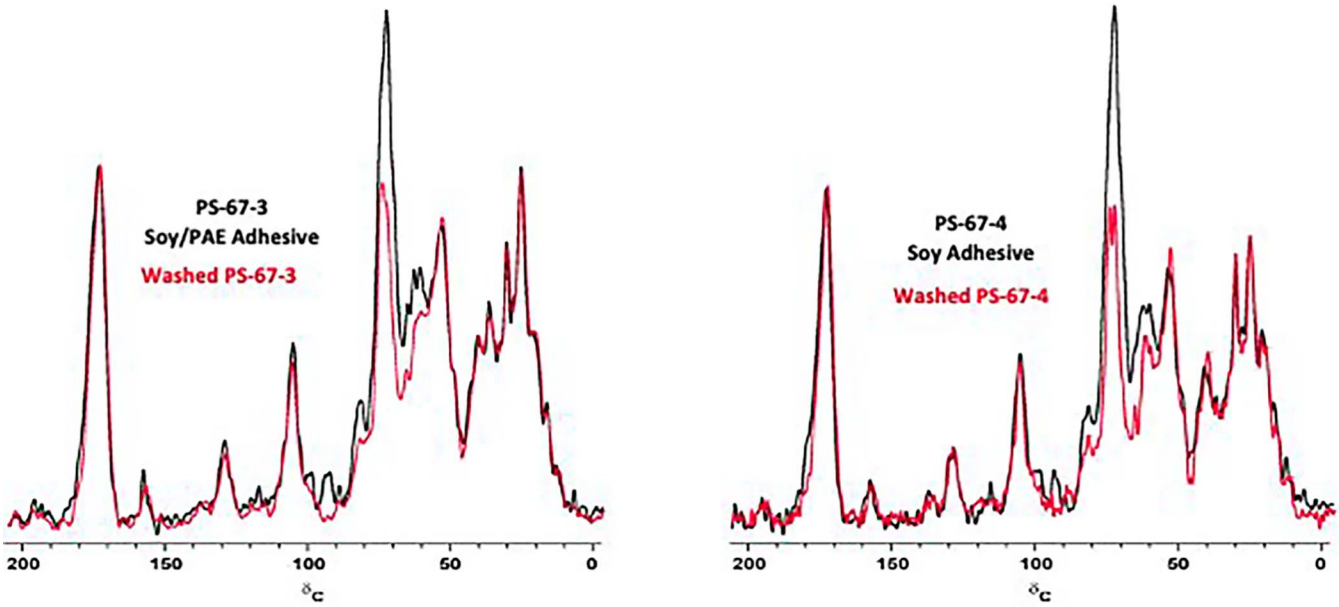

Figure 4.—Overlays of the ^{13}C cross-polarization-magic angle spinning (CP-MAS) spectra for dried adhesive film samples 67-3 and 67-4 before washing (black) and after water soaking–washing (red).

water-soluble components of soy flour. Our findings will be published soon.

Interestingly, an opposite trend was observed in the absence of PAE (67-4). Upon removal of the water-soluble fraction from 67-4, the $^{1}HT_{1\rho}$ values were observed to increase after soaking–washing, indicating that molecular motion was enhanced upon removal of the water-soluble fraction. Thus, in the absence of PAE, the presence of the water-soluble fraction was observed to inhibit molecular motion before washing–soaking, and after its removal, molecular motion increased dramatically.

This unique finding illustrates that PAE not only has an influence on the composition of the water-soluble fraction as observed via FTIR, but it also has an influence on the molecular dynamics of the water-soluble fraction, which translates to an effect on the physical properties and molecular mobility of the adhesive molecules. This finding has justified further characterization of the water-soluble fractions using 2-dimensional NMR techniques, a pursuit that is presently in progress within our laboratories.

In summary, from these comparisons of the samples (i.e., before and after washing), it appears that PAE inhibits the molecular mobility of the water-insoluble residue. This finding is in line with traditional expectations from crosslinking reactions. However, the effect of PAE on the water-soluble fraction is counterintuitive, in that the water-soluble fraction appears to plasticize the adhesive when PAE is employed in the formulation, whereas in the absence of PAE, the water-soluble fraction retards the molecular motions, and thus contributes to the rigidity of the system.

It should be mentioned that these trends are consistent with qualitative observations pertaining to the mechanical characteristics of water-soluble fractions after drying. In the presence of PAE, the water-soluble extract was observed to be mechanically compliant and tacky, whereas in the absence of PAE, the extract was observed to be glassy and brittle. Further NMR analyses as well as thermomechanical analyses are currently underway for the purpose of quantifying structural differences as well as physical property differences between the extracts.

Implications and Conclusions

The FTIR and SSNMR data suggest that PAE interacts in an unusual way with the soluble portions of the soy flour. The water-soluble reaction product or mixture not only becomes tacky and plasticized, but it also appears to become concentrated on the surface of the adhesive, rendering it

Table 1.—Proton Spin Lattice Relaxation in the Rotating Frame ($^{1}HT_{1\rho}$) molecular relaxation data as measured through carbon for adhesive samples 67-3 and 67-4 before and after washing. The relaxation rates are given in milliseconds (ms).

NMR Peaks (ppm)	67-3 Soy /PAE Adhesive $^{1}HT_{1\rho}$ (ms)	Washed 67-3 Soy/PAE Adhesive $^{1}HT_{1\rho}$ (ms)	67-4 Neat Soy Adhesive $^{1}HT_{1\rho}$ (ms)	Washed 67-4 Neat Soy Adhesive $^{1}HT_{1\rho}$ (ms)
173	5.9	3.5	6.3	8.6
129	5.3	3.8	7.2	8.3
104	5.1	3.8	6.1	14.6
72	5.3	4.0	5.1	11.7
62	4.6	4.0	6.1	10.3
30	5.6	3.9	6.7	8.8
24	6.0	3.7	6.7	9.0

Note: Error associated with the measurements ranged between 0.05 - 0.2 ms.

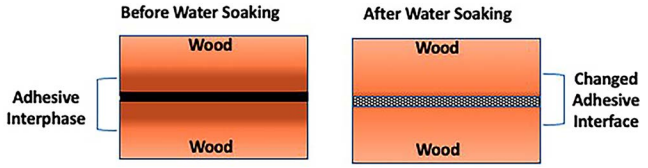

Figure 5.—Hypothesized adhesion mechanism for Soy–PAE adhesives and how the bond-line changes when laminated composites are exposed to water.

available for preferential penetration into the porous wood adherend during the lamination process. This hypothesis is pictorially illustrated in Figure 5.

In one regard, the penetration of the water-soluble components into the adherend could have a positive benefit. For example, penetration would yield a blended interphase region between wood components and adhesive components. The presence of an interphase of this type would be expected to have a positive impact on interfacial stress dissipation, energy absorption, and ultimate bond strength (Theocaris 1987).

When the adhesive is cured with PAE, it seems to benefit from the effects of a crosslinking reaction, as evidenced by a decrease in molecular motions. However, the water-soluble surface components are moisture-sensitive and qualitatively low in modulus. Thus, in the presence of moisture, an interphase that preferentially consists of these water-soluble components would become susceptible to moisture ingress and to dissolution, leading to the formation of a weak boundary layer. In turn, this would lead to a lower capacity for stress dissipation, and to a higher propensity for water-induced delamination failures as are routinely observed with these types of adhesives.

In addition, water-soluble components are also present within the bulk adhesive, and they are also subject to extraction upon exposure to moisture; therefore, the bulk adhesive within the center of the bond-line would have the propensity to lose mass, which could lead to defect sites that are susceptible to crack propagation, possibly exasperated by the fact that the rigidity and stiffness of the bond-line material increases upon extraction of the water-soluble components.

We are presently using NMR imaging techniques to test these adherend penetration hypotheses, and 2-D NMR techniques to structurally analyze the differences in water-soluble components as a function of the presence and absence of PAE. We are also using FTIR and NMR to study extracts from the wood adherends themselves, in the presence and in the absence of adhesives. In addition, we are using thermomechanical analysis techniques to study the effects of PAE on the mechanical properties of the water-soluble and insoluble components.

The goal of these studies will be to identify the chemical nature and mechanistic role of the water-soluble components during the various stages of use, including during mixing (e.g., water-phase chemistry), during the lamination process (e.g., diffusion into the adherend), and after lamination (e.g., composition of the interphase). By developing a better mechanistic understanding, it should be possible to develop targeted solutions aimed at enhancing the moisture resistance of these soy-based adhesive systems.

Further reporting of the chemistry and properties of the water-soluble extractable material is forthcoming.

Acknowledgments

The authors would like to thank the United Soy Board for funding this research (Project Number: 2333-101-0101). We thank Columbia Forest Products for providing the 200/70 soy flour, the PAE resin, and the wood veneers for these studies. We also thank Dr. Anil Mehta and the staff from the University of Florida, McKnight Brain Institute at the National High Magnetic Field Laboratory's Advanced Magnetic Resonance Imaging and Spectroscopy (AMRIS) Facility, for their assistance with the solid-state NMR studies. The facility is supported by National Science Foundation Cooperative Agreement DMR- 1644779 and the State of Florida. This work was also supported in part by an National Institute of Health award, S10 OD028753, for magnetic resonance instrumentation.

Literature Cited

Adamson, A. W. 1990. Physical Chemistry of Surfaces. Fifth ed. John Wiley & Sons, Inc., New York. pp. 460–489. ISBN 0-471-61019-4.

Allen, A. J., J. J. Marcinko, T. A. Wagler, and A. J. Sosnowick. 2010. Investigations of the molecular interactions of soy based adhesives. *Forest Prod. J.* 60(6):534–540. https://doi.org/10.13073/0015-7473-60.6.534

Bello, D. 2006. An FTIR investigation of isocyanate skin absorption using in vitro guinea pig skin. *J. Environ. Monit.* 8:523–529.

Erickson, D. R. (Ed.). 1995. Practical Handbook of Soybean Processing and Utilization. AOCS Press, Urbana Illinois, and United Soy Board, St. Louis Missouri.

Frihart, C. R. and M. Birkeland. 2016. Soy products for wood binding. *In:* Forest Resource and Products: Moving Toward a Sustainable Future. Proceedings of the 59th International Convention of Society of Wood Science and Technology, LeVan-Green, S. (Ed.), March 6–10, 2016, Curitiba, Brazil. pp. 192–199.

Guillemenet, J., S. Bistac, and J. Schultz. 2002. Relationship between polymer viscoelastic properties and adhesive behaviour. *Int. J. Adhes. Adhes.* 22(1):1–5.

Hunt, C. G., L. F. Lorenz, C. J. Houtman, E. Valle, T. Coolidge, C. Mock and C. R. Frihart. 2023. Jet cooking dramatically improves the wet strength of soy adhesives. *J. Am. Oil Chem. Soc.* 100(1):69–79. https://doi.org/10.1002/aocs.12664

Koenig, J. L. 1999. Spectroscopy of Polymers. Second ed. Elsevier Inc., New York. 112 pp.

Korb, J. and R. G. Bryant. 2004. Magnetic field dependence of proton spin-lattice relaxation of confined proteins. *Magn. Reason. Med.* 48(1):21–26.

Li, K. 2007. Formaldehyde-free lignocellulosic adhesives and composites made from the adhesives. US patent 7,252,735. https://patentimages.storage.googleapis.com/2a/28/6c/7ce2af790f567f/US7252735.pdf. Accessed January 22, 2024.

Li, K., S. Peshkova, and X. Geng. 2004. Investigation of soy proteinkymene adhesive systems for wood composites. *J. Am. Oil Chem. Soc.* 81(5):487–491.

Li, K. and L. Yuan. 2006. Modified protein adhesives and lignocellulosic composites made from the adhesives. US patent 7,060,798. https://patentimages.storage.googleapis.com/36/d0/38/7e9e83c0f5d8f9/US7060798.pdf. Accessed January 22, 2024.

Marcinko, J. et al. 2003. Solid state two-dimensional NMR studies of polymeric diphenylmethanediisocyanate (PMDI) reaction in wood. *Forest Prod. J.* 53(6):63–71

McBrierty, V. J. and D. C. Douglass. 1981. Recent advances in the NMR of solid polymers. *J. Poly. Sci.: Macromol. Rev.* 16(1):295–366.

Parker, A. A. 2002. The effect of silane hydrolysis on aluminum oxide dispersion stability in ceramics processing. *J. Adhes. Sci. Tech.* 16(6): 679–701.

Parker, A. A. 2004. Musical instrument strings and corrosion: A comparative study of aminosilane and benzotriazole surface treatments. *In:* Silanes and other Coupling Agents, Volume 3. K. L. Mittal (Ed.). VSP BV, The Netherlands. pp. 161–176.

Parker, A. A. and J. MacLachlan. 2000. The relationship between silane hydrolysis and polymer adhesion to glass as studied by 13C solid state

NMR. *In:* Silanes and Other Coupling Agents, Volume 2. K. L. Mittal (Ed.). VSP BV, The Netherlands. pp. 27–40.
Parker, A. A., S. M. Opalka, N. R. Dando, D. G. Weaver, and P. L. Price. 1993. Studies of polymer mobility in composite blends of poly(vinyl-butyral) and alumina. *J. Appl. Polym. Sci*. 48(10):1701–1707.
Parker, A. A., J. Sun, A. M. Ahern, T. Stanzione, D. Wilhelmy, G. H. Armstrong, and J. J. Marcinko. 1992. Effect of dispersion state on ceramic green body morphology. *Polym. Prepr*. 33(1):1210.
Schaefer, J., J. R. Garbow, E. O. Stejskal, and J. A. Lefelar. 1987. Plasticization of poly(butyral-covinyl alcohol). *Macromolecules* 20(6):1271–1278.
Theocaris, P. S. 1987. Synergism phenomena between phases in composites: The mesophase. *Colloid Polym. Sci*. 265:461–480.
Watt, C. 2008. Developing soy-based adhesives for composite panels. Presented at the 42nd International Wood Composites Symposium, March 31–April 2, 2008, Seattle, Washington. Forest Products Society, Madison Wisconsin.